MBNA Publishing House Constanta 2021

Proceedings of the International Scientific Conference SEA-CONF

SEA-CONF PAPER • OPEN ACCESS

Some analytical methods used to process research drawing - Part II

To cite this article: Aurelia CHIOIBAS, Proceedings of the International Scientific Conference SEA-CONF 2021, pg.27-36.

Available online at www.anmb.ro

ISSN: 2457-144X; ISSN-L: 2457-144X

doi: 10.21279/2457-144X-21-004

Some analytical methods used to process research drawing - Part II

A CHIOIBAS

"Mircea cel Batran" Naval Academy
chioibasaura@yahoo.com

Abstract. This paper refers to several other analytical methods used in the research of drawing, other than the classic.

Keywords: sliding lines, finite element method

Introduction

The research of the stamping process was performed with both analytical and experimental methods. In the category of analytical methods for drawing research, in a previous paper was presented the method of solving equilibrium equations [6], and in this paper will be presented two other methods used for this purpose.

1. The sliding line method

In the case of a solid body subjected to a flat stress state, at any point on a surface inclined to an xOy coordinate system, two normal stresses and one tangential will act. For a certain position of the surface it can be like $\tau = 0$ and as a result the normal stresses have extreme values, called main normal stresses (σ_1, σ_2) [4].

As a result, for any point inside a semi-finished product subjected to deformation, there are two perpendicular directions on which the unit forces σ_1 and σ_2 act and two other directions inclined with respect to the first by 45°, after which $\tau_{max} = K$ acts. Under these conditions, taking into account different points on the surface of the material to be processed, a network consisting of two systems of curves will be obtained, at which the tangents have the direction of the main normal stresses. In relation to these two systems, two other curve systems can be built, in which the tangents have the direction of the maximum tangential stresses (Fig. 1).

By processing the relations that give the plane state of efforts [1] we arrive at the differential equations of the sliding lines:

$$\sigma_x = \frac{\sigma_1 + \sigma_2}{2} + \frac{\sigma_1 - \sigma_2}{2}\cos 2\varphi \ ; \tag{1}$$

$$\sigma_y = \frac{\sigma_1 + \sigma_2}{2} - \frac{\sigma_1 - \sigma_2}{2}\cos 2\varphi \ ; \tag{2}$$

$$\tau_{xy} = \frac{\sigma_1 - \sigma_2}{2} \sin 2\varphi \ . \tag{3}$$

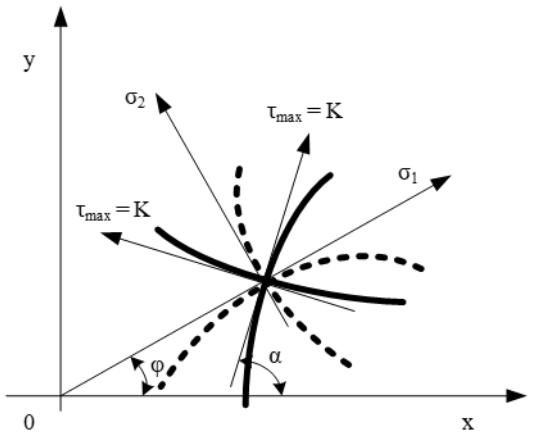

Fig.1. The network consists of two systems of curves corresponding to the unitary efforts and other two systems that correspond to the maximum tangential stresses

Taking into account the relationships:

$$\sigma_{med} = \sigma_0 = \frac{\sigma_1 + \sigma_2}{2}; \tag{4}$$

$$K = \frac{\sigma_1 - \sigma_2}{2}; \tag{5}$$

$$\varphi = \alpha - \frac{\pi}{4}. \tag{6}$$

equations (1) - (3) become:

$$\sigma_x = \sigma_{med} + K \cdot \sin 2\alpha; \tag{7}$$

$$\sigma_y = \sigma_{med} - K \cdot \sin 2\alpha; \tag{8}$$

$$\tau_{xy} = -K \cdot \cos 2\alpha. \tag{9}$$

The tangents to the sliding lines have the directions of $\tau_{max} = K$. They intersect the axis Ox under the angles α and $(\alpha + \pi / 2)$. As a result, the differential equations of the sliding lines are:

$$\left(\frac{dy}{dx}\right)_1 = tg\alpha; \tag{10}$$

$$\left(\frac{dy}{dx}\right)_2 = tg\left(\alpha + \frac{\pi}{2}\right). \tag{11}$$

Integration of the plasticity equation

Inside a body subjected to a state of flat stress, an O point is considered, through which two mutually perpendicular sliding lines pass (Fig. 2. [1]). In the xOy coordinate system, the tangent T taken to the sliding line ξ, forms the angle α with the axis Ox. It is known that along the sliding lines, the tangential stresses are maximum and remain constant.

It is considered a volume element in the shape of a triangular prism, arranged so that the inclined surface ΔA is tangent to the sliding line ξ at point O and the other two surfaces are perpendicular to

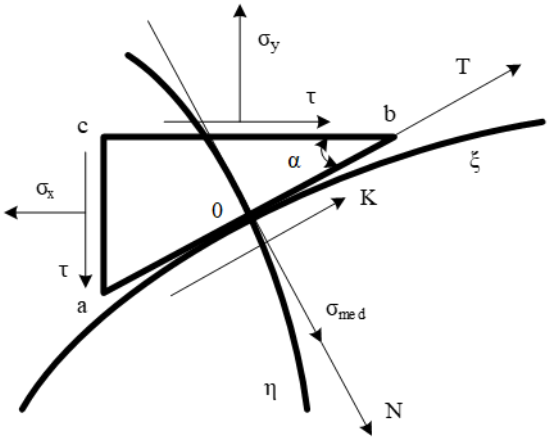

Fig. 2. Representation of the volume element, of the sliding lines, necessary to understand the integration of the plasticity equation

the coordinate axes. The aim is to determine the value of the average normal voltage, reason for which the projections of the forces in the direction of the normal N are made, obtaining:

$$\sigma_{med} dA = \sigma_y dA_y \cos\alpha + \sigma_x dA_x \sin\alpha - \tau dA_x \cos\alpha - \tau dA_y \sin\alpha \quad (12)$$

Considering that:

$$dA_x = dA \cdot \sin\alpha; \quad (13)$$

$$dA_y = dA \cdot \cos\alpha; \quad (14)$$

result: $$\sigma_{med} = \sigma_y \cos^2\alpha + \sigma_x \sin^2\alpha - \tau \sin 2\alpha . \quad (15)$$

Differentiating the relation (15) in relation to α we obtain:

$$\frac{d\sigma}{d\alpha} = (\sigma_x - \sigma_y) \cdot \sin 2\alpha - 2 \cdot \tau \cdot \cos 2\alpha \quad (16)$$

From relationships (7) - (9), (16) result:

$$d\sigma_{med} = 2Kd\alpha \quad (17)$$

When the hypotenuse "ab" coincides with the sliding direction η, will result in the relationship 17.

Therefore, in the general case it is considered:

$$d\sigma_{med} = \pm 2Kd\alpha . \quad (18)$$

Integrating the differential equation (18), along the sliding line, from point "a" to point "b", we obtain:

$$\sigma_a - \sigma_b = \pm 2K(\alpha_a - \alpha_b) \text{ or } \sigma_a - \sigma_b = \pm 2K\alpha_{ab} . \quad (19)$$

The relation (19) represents the integral of the plasticity equation or the integral of Hencky and shows that if we know (σ_a) - the average normal stress at point "a" and (α_{ab}) - the angle of rotation of the sliding lines from "a" to in "b", the value of the average normal stress acting at point "b" can be determined.

In order to construct the network of sliding lines when drawing a cylindrical part (Fig. 3 [1], [21]), it is observed that at a certain point in the flange of the semi-finished product the radial tension σ_ρ and the tangential tension σ_t arise, which are intersected by the sliding lines under a angle of 45°.

So: $$d\rho = \rho d\varphi \Rightarrow d\varphi = \frac{d\rho}{\rho} \Rightarrow \varphi = \ln\rho + C \Rightarrow \alpha_{ab} = \varphi_{ab} = \ln\frac{D}{d} = \ln\frac{R}{r} \quad (20)$$

Equation (18) becomes:

$$\sigma_{med_a} - \sigma_{med_b} = 2K \ln \frac{R}{r}. \tag{21}$$

In point "b", we have:

$$\sigma_{\rho b} = 0,\ \tau_{max} = (\sigma_{\rho_b} - \sigma_{t_b})/2 = K \Rightarrow \sigma_{med_a} = (\sigma_{\rho_a} + \sigma_{t_a})/2 = -K. \tag{22}$$

In point "a", we have:

$$\sigma_{\rho a} - \sigma_{ta} = 2k \Rightarrow \sigma_{med_a} = (\sigma_{\rho_a} + \sigma_{t_a})/2 = \sigma_{\rho_a} - K. \tag{23}$$

From the last three relations it results:

$$\sigma_{\rho a} = 2K \ln \frac{R}{r}. \tag{24}$$

For $K = 0.5 \cdot \sigma_c$ and a certain radius ρ, the stress required for deep drawing becomes:

$$\sigma_{\rho} = \sigma_c \ln \frac{R}{r}. \tag{25}$$

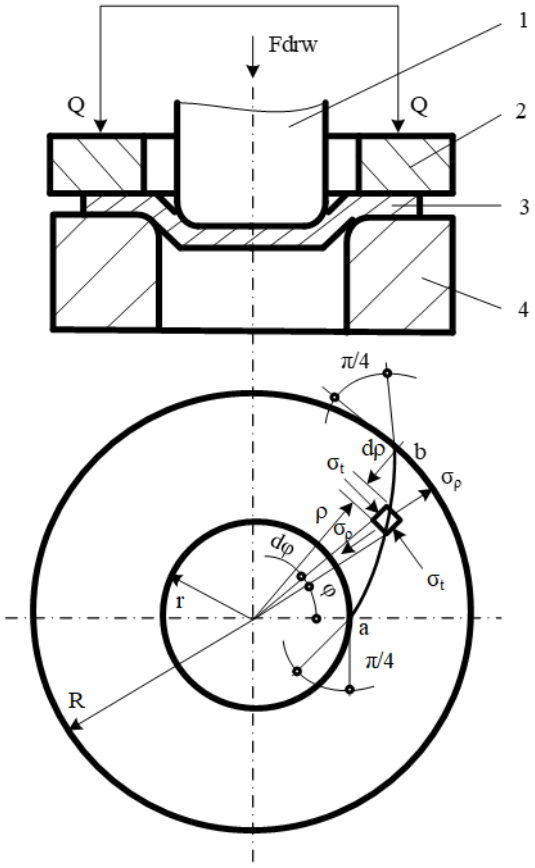

Fig. 3.. Representation of the state of tension and of the sliding line at a certain point in the flange of the semi-finished product

2. FEM

In ([17], [21]) a presentation of the finite element method (FEM) is given. Initially, the two types of approximations are defined: non-nodal and nodal. For this we know some values of the exact function uex in some points and to determine the values it takes in other points it is necessary to construct an approximate function of the form u (x, a_1, ..., a_n) so that:

$$u(x) = P_1(x)a_1 + \ldots + P_n(x)a_n \;\Leftrightarrow\; u(x) = \langle P_1(x) \ldots P_n(x) \rangle \begin{Bmatrix} a_1 \\ \vdots \\ a_n \end{Bmatrix} = \langle P \rangle \{a\} \tag{26}$$

$$\text{and } u_{ex}(x) = u(x) \Rightarrow (a_1 \ldots, a_n),$$

where: a_i represents the general parameters of the approximation; with P(x) the basic functions of the approximation were noted; the relations (26) correspond to the non-nodal approximation.

If the approximation error $e(x) = u(x) - u_{ex}(x) = 0$ in any node xi, then the nodal parameters (nodal variables) are obtained $u_{ex}(x_i) = u(x_i) = u_i$ and the relation (26) becomes:

$$u(x) = N_1(x)u_1 + \cdots + N_n(x)u_n \quad \text{or} \quad u(x) = \langle N_1(x) \cdots N_n(x) \rangle \begin{Bmatrix} u_1 \\ \vdots \\ u_n \end{Bmatrix} = \langle N \rangle \{u\}, \tag{27}$$

wherein the relations (27) correspond to the nodal approximation and N(x) represent interpolation functions that verify the relation:

$$N_i(x_j) = \begin{cases} 0, & \text{if } i \neq j \\ 1, & \text{if } i = j \end{cases} \tag{28}$$

In the case of a Lagrange nodal approximation with "n" points, the relation (28) becomes:

$$N_i(xj) = \prod_{\substack{j=1 \\ i \neq 1}}^{n} \frac{(x - x_j)}{(x_i - x_j)}. \tag{29}$$

For domains of complex shape with a large number of nodes, the approximation is made with the finite element, which involves the analytical definition of all subdomains into which the initial domain was divided (elements) and the construction of interpolation functions $N_i(x)$, corresponding to each finite element. The notion of reference element, V^r, is introduced, which has a simple shape and is in a reference space and which can be transformed into any of the real elements V^e by a geometric transformation (Fig.4 [17]) of the form:

$$\tau : \xi \rightarrow x(\xi);\; x(\xi) = \left[\overline{N}(\xi)\right]\{x_n\}, \tag{30}$$

in which $\overline{N}$ the functions of geometric transformation have been noted, which are polynomials as a function of ξ and are constructed similarly to the functions of interpolation N(ξ).

In the space (x, y) we worked with the approximation function u(x), and in the space (ξ, η) we worked with the function u(ξ, η), the relation between ξ and x being defined by (30). The functions $u(\xi) \neq u(x)$, but take the same value at the corresponding points by transformation.

To construct the N (ξ) functions and the coordinate vector of each element $\{x_n\}$, two tables are drawn up: CORG and CONEC. CORG contains all the geometric nodes (1, 2, ..., n) provided with the nodal coordinates $[(x_1 y_1) \cdots, (x_n y_n)]$, and CONEC contains all the elements $(1, 2, \cdots, \overline{n}_{el})$ defined by the list of numbers of the geometric nodes (1, 2, ..., n^e). In order to establish the list of nodes of an element, it is necessary to adopt a direction of movement of the element.

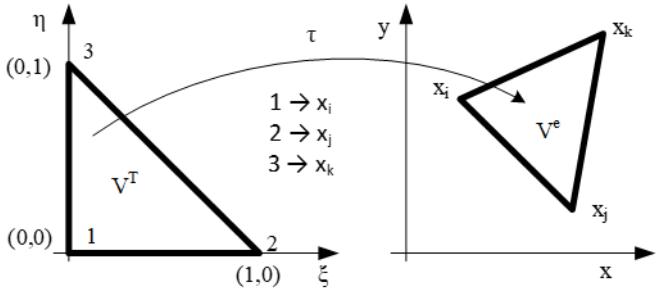

Fig. 4 . The reference element V^T and the real element V^e obtained by the geometric transformation τ

Tabel 1. The table CONEC

Elements	List of geometric node numbers
1	1……. n^e
2	..
..	..
..	..
$\overline{n}_{el}$	n_1…… n_n^e

Tabel 2. The table CORG

Knots	Nodal coordinates	
1	x_1	y_1
2	x_2	y_2
..	..	..
..	..	..
..	..	..
n	x_n	y_n

For "n" interpolation nodes with x_n coordinates (which may or may not be confused with geometric nodes) located on the real element V^e and an exact function $u_{ex}(x)$, a nodal approximation of the form (27) can be constructed, ie:

$$u_{ex}(x) \approx u(x) = \langle N(x) \rangle \{u_n\}, \tag{31}$$

in which: $\{u_n\} = u_{ex}(x_n)$ represent the nodal variables and the interpolation functions on the real element V^e were denoted by N(x).

Is used on the reference element V^r a nodal approximation u_{ex} (ξ) having the form:

$$u_{ex}(\xi) \approx u(\xi) = \langle N(\xi) \rangle \{u_n\}, \tag{32}$$

wherein N (ξ) represents the interpolation functions on the reference element V^r.

While the functions N(x) depend on the coordinates of the nodes of the element, so they differ from one element to another, the functions N(ξ) are independent of the geometry of the real element V^e, so they can be used for all elements with the same element of reference characterized by: its shape, its geometric nodes, its interpolation nodes. There is no systematic manual technique for constructing N(ξ) and $\overline{N}(\xi)$ functions, but experience has allowed them to be found for a number of classical elements. They have the same properties and are constructed from Lagrange polynomials. The general construction method includes the following steps:

a) Choosing the polynomial basis

On the reference element V^r is expressed $u(\xi)$ as a linear combination of known functions (generally independent monomials) $P_1(\xi), \ldots, P_n(\xi)$, of the form:

$$u(\xi) = \langle P_1(\xi) \ldots P_n(\xi) \rangle \begin{Bmatrix} a_1 \\ \vdots \\ a_n \end{Bmatrix} = \langle P(\xi) \rangle \{a\}. \tag{33}$$

The above relation corresponds to the generalized approximation. In this relation was noted the generalized variables of the element with "a_n" and the nodal approximation with $u(\xi) = \langle N(\xi) \rangle \{a\}$. The number of functions $P(\xi)$ is equal to the number of nodal variables ($\{u_n\}$) and they form the polynomial basis of the approximation, which can be complete or incomplete.

To build the function $\overline{N}$ are chosen:

$$\begin{aligned} x(\xi) &= \langle \overline{P}(\xi) \rangle \{a_x\} \\ y(\xi) &= \langle \overline{P}(\xi) \rangle \{a_y\} \\ z(\xi) &= \langle \overline{P}(\xi) \rangle \{a_z\} \end{aligned} \tag{34}$$

where $\{a_x\}$, $\{a_y\}$, $\{a_z\}$ represent the generalized coordinates of the element.

b) Relationships between generalized variables $\{a\}$ and nodal variables $\{u_n\}$

In each interpolation node (ξ_i) the relation $u_{ex}(\xi) \approx u(\xi) = u_i$ is valid and taking into account (33) we obtain:

$$\{u_n\} = \begin{bmatrix} P_1(\xi_1) & P_2(\xi_1) & \cdots & P_n(\xi_1) \\ P_1(\xi_2) & P_2(\xi_2) & \cdots & P_n(\xi_2) \\ P_1(\xi_n) & P_2(\xi_n) & \cdots & P_n(\xi_n) \end{bmatrix} \{a\} \Leftrightarrow \{u_n\} = [P_n]\{a\} \Rightarrow \{a\} = [P_n]^{-1}\{u_n\}; \tag{35}$$

$$\left(\exists [P_n]^{-1} \text{ if } \det(P_n) \neq 0\right)$$

The relation (34) written in the geometric nodes becomes:

$$\begin{aligned} \{x_n\} &= [\overline{P}]\{a_x\} \qquad \{a_x\} = [\overline{P}_n]^{-1}\{x_n\} \\ \{y_n\} &= [\overline{P}]\{a_y\} \text{ or } \{a_y\} = [\overline{P}_n]^{-1}\{y_n\} \\ \{z_n\} &= [\overline{P}]\{a_z\} \qquad \{a_z\} = [\overline{P}_n]^{-1}\{z_n\} \end{aligned} \tag{36}$$

c) Expressions of the functions N and $\overline{N}$

From the relations (33) and (35) results:

$$\left.\begin{aligned} u(\xi) &= \langle P(\xi) \rangle [P_n]^{-1}\{u_n\} \\ u(\xi) &= \langle N(\xi) \rangle \{u_n\} \end{aligned}\right\} \Rightarrow \langle N(\xi) \rangle = \langle P(\xi) \rangle [P_n]^{-1} \tag{37}$$

From the relations (34) and (36) results:

$$\left.\begin{aligned} x(\xi) &= \langle \overline{P}(\xi) \rangle \{a_x\} = \langle \overline{P}(\xi) \rangle [\overline{P}_n]^{-1}\{x_n\} \\ y(\xi) &= \langle \overline{P}(\xi) \rangle \{a_y\} = \langle \overline{P}(\xi) \rangle [\overline{P}_n]^{-1}\{y_n\} \\ z(\xi) &= \langle \overline{P}(\xi) \rangle \{a_z\} = \langle \overline{P}(\xi) \rangle [\overline{P}_n]^{-1}\{z_n\} \\ x(\xi) &= [\overline{N}(\xi)]\{x_n\} \end{aligned}\right\} \Rightarrow \overline{N}(\xi) = \langle \overline{P}(\xi) \rangle [\overline{P}_n]^{-1} \tag{38}$$

These operations are performed once for all real elements, which have the same reference element.

The assembly of the element equations for obtaining the equations on the whole domain of work can be done by the following methods: direct integration of the system equations; determination of external forces and moments, when stresses or deformations are known; solving a system of simpler equations, when entering experimentally obtained data.

3. Application of these analytical methods of research of the drawing process

In [17] the program finite element FORGE2 is presented.

The finite element method is the most used method for modeling sheet metal deformation processes, for determining the drawing limit curves ([15], [23]), or for determining their deformability. Also, this method allows the optimization of cold plastic deformation processes, including drawing [10]. In [3] is presented a way to analyze the deep drawing process using the finite element method, which aims to solve the nonlinear geometric problem of plasticity theory with the finite element method, the modified Lagrange formulation and the Newton - Raphson method. Also for deep drawing, in [20] is presented an algorithm for numerical integration of the relations corresponding to the finite deformations of an anisotropic elastoplastic material. The mathematical model takes into account the friction between the punch, the plate and the active plate, the punch can have any shape. The exemplification was made on a cylindrical box and there is a good concordance between the values of the stresses obtained experimentally and numerically.

The finite element method is also used to determine the deformability of sheets ([12], [16]), which is an important feature for the correct assessment of the use of semi-finished products in order to obtain quality parts. In [19] a study on the plastic instability that occurs during deformation is presented. Thinning of the sheet occurs when there are unevenness of the deformation speed. After the appearance of static instability, the direction of deformation can no longer be controlled as until the moment of its appearance. At the end of the process, a local thinning occurs because the process satisfies the conditions of kinematic instability.

The study of the influence of some factors on the coefficient of friction at the deep drawing of the parts is presented in the paper [22]. The factors considered are: the degree of drawing, the pressure on the contact surface ([2], [22]), the dimensions of the semi-finished product, its initial thickness. The research method used to determine the coefficient of friction by solving on the computer the equations of the drawing stresses by Müller's method is described.

The method of determining the critical load and the limit coefficient for deep drawing of cylindrical parts is given in [7]. The research of the loss of the stability of the flange of the semi-finished product and of the appearance of the corrugations with the formation of wrinkles at the stamping is presented in ([24], [25]).

The drawing with the deliberate thinning of the wall thickness of the anisotropic materials is presented in [13], and the choice and use of materials for this process is presented in [11]. In [18] the case of obtaining food beverage containers by deep drawing with thinning of the thickness of the semi-finished steel and aluminum sheet is presented. The studied problems were: lubrication, crack formation and prevention of their appearance, removal of the piece from the punch, cutting the edges. The obtained results allow to increase the precision of the parts and to optimize the choice of the material from which the mold is made.

In [9] the theoretical analysis of the stress state is performed depending on the force applied on the deformed material, in case of successive stamping with thinning of the wall. The formulas for the calculation of stresses, forces and the permissible degree of deformation limit when stamped with a conical and cylindrical punch in one or more successive dies are presented. The limit deformation control mechanism is established, which specifies the ways to intensify the drawing processes as the friction conditions are adjusted on the surface of the mold and the angles of inclination of the molds. The concordance of the calculation results with the experimental data led to the design of the technological processes for drawing the deep cavities.

A research on the compatibility of tool and semi - finished material when drawing metal sheets is presented in [8].

In [14] is presented a methodology for determining the number of passes required for drawing, the drawing coefficient for the second and subsequent operations required to obtain cylindrical parts. The basis of this methodology are the equations of the theory of plasticity and the theory of minimax, whose application allows the prediction of the influence of technological drawing regimes and mechanical properties of the material on the drawing limit coefficient. This methodology contains a program that allows the establishment of the limits of the range of values of the drawing coefficient for each passage, aspect that is the basis for the design of the technological process of manufacturing the parts.

Using software designed on the finite element method (COSMOS, LS-DYNA, MARC-Mentat) it was possible to analyze the state of stresses and deformations [5] that arises from the stamping of small cylindrical parts, obtained from strips of different materials, characterized of different plasticities.

References

[1] Banabic D., Dorr I. R., 1992, *Deformabilitatea tablelor metalice subţiri,* Bucureşti

[2] Blümel W.K., *Interacţiunile de suprafaţã în timpul prelucrãrii prin deformare, conform simulãrii pe baza încercãrii de ambutisare pe bandă metalicã,* Sheet Metal Industries, februarie 1980, pag. 152 – 160

[3] Brunet M., *A finite element method for a numerical analysis of the deep-drawing process* , Proc. Int. Conf. Numer. Math. Eng.: Theory and Appl. Swansea, 6-10 July, 1987, Numeta 1987, vol. 1

[4] Cazimirovici E., 1982, *Teoria deformării plastice,* Editura Tehnică, Bucureşti

[5] Chioibas A., 2004, *Cercetari privind influenta conditiilor de deformare asupra calitatii pieselor ambutisate,* Bucuresti

[6] Chioibas A., *Some analytical methods used to process research drawing - Part I*, Journal of Physics: Conference Series, Volume 1122, conference 1, IOP Conf. Series: Journal of Physics: Conf. Series 1122 (2018)

[7] Deng Z., Chen H., *Sheet metal formability using the FEM,* J.Tsinghua Univ., 1989, nr.2

[8] Dohda K., Kawai N., *Compatibility between tool materials and workpiece in sheet-metal ironning process,* Trans. ASME. J. Tribol., 1990, nr.2

[9] Doroşko V.I., 1990-24, *Analiz proţessa posledovatelinoi vîtiajki s utoneniem stenki,* Lugan. Maşinostroit. In-t-Lugansk, p. 274-281

[10] Drăgănescu F., ş.a., *Cercetări privind optimizarea proceselor de prelucrare prin deformare plastică la rece folosind simularea numerică cu ajutorul M.E.F***.** Bucureşti 1991

[11] Gadzinski S., *Wykorzystanie materialu w procesie Hoczenia cienkosciennych wyrobov cylindrycznych,* Obrob. Plast. Metali., 1989, nr.3

[12] Ghuida M., Porraro G., *Applicatione di una metodologia di calcole FEM alla previsione della stampabilita della lamiera,* Lamiera-1990, 27, nr.1

[13] Iakovlev S.S., Arefiev Y.M., *Vîtiaka s utoneniem stenku anizotropnovo uprociniaiuscegosia materiala,* Tul. Politehn.in-t-Tula, 1989

[14] Iseki H., Sowerby R., , 1990, *On the determination on the redrawing ratio in the redrawing of cilindrical sheels with a numerical simulation,* J. ASME Int. J. Ser. 3, nr.2, p. 376-384

[15] Josselin H., *Studiul C.L. de formare prin ambutisare,* Formageet traitements de métaux, nr. 27, 1971

[16] Kobayashi S., ş.a. *Analysis of a Test Method of Sheet Metal Formability Using the Finite Method* Journal of Engineering for Industry, 1986, nr. 1

[17] Maier C., 2003, *Proiectarea tehnologică asistată de calculator,* Editura Evrika, Brăila

[18] Misono K., *Generalized finite element analysis of sheet metal forming with an elastic-*

viscoplastic material model, Technol. Repts. Kyushu. Univ., 1989, nr.6
[19] Moritoki H., *Simulating the sheet metal forming pocess with FEM,* Trans. Jap**.** Soc. Mech. Eng., 1990, nr.56
[20] Sarah M., ş.a. *Numerical integration of finite deformation elasto plasticity with application to sheet-forming,* Comput. Mech. 1988: Theory and Appl.: Proc. Int. Conf. Comput. Eng. Sci. Atlanta. 10-14, 1988. vol. 2
[21] Teodorescu M., ş.a., 1987, *Prelucrări prin deformare plastică, vol. I, II*, Editura Tehnică, Bucureşti
[22] Vedmedi I.P., Verşinin V.A, *Issledovanie na EVM ne katorîh factorov vliiaiuscîh na koeffiţient treniia pri glubokai vtiajke detalei***,** Red. J. Tehnol. I Org. Pr-vo Kiev, 1990
[23] Veerman C.Chr., Neve P.F., *Câteva aspecte ale determinării CLA – începutul gâtuirii localizate,* Sheet Metal Industries, 49, nr. 6, iunie 1972, pag. 421 – 423
[24] Wang P.C., *A Wrinkling index for press forming,* Met. Trans. A.,1988, nr.7-12
[25] Wang X., Lee L., *Wrinkling of an unevenly stretched sheet metal,* Trans. Asme. J. Eng. Mater. and Technol., 1989, nr.3